JOURNAL OF COMPUTATIONAL PHYSICS 44, 167–188 (1981)

Numerical Treatment of Nonconservation Forms of the Equations of Shallow Water Theory

GUILLERMO MARSHALL*

Consejo Nacional de Investigaciones Científicas, Buenos Aires, Argentina

AND

ANGEL N. MENÉNDEZ†

Laboratorio de Hidráulica Aplicada, INCYTH, Buenos Aires, Argentina

Received August 18, 1980; revised February 20, 1981

Nonconservation forms of the equations of shallow water theory are solved by an extension of the Random Choice Method. The nonconservation Riemann problem is analyzed in terms of two nonlinearly interacting waves and is solved by means of a numerical integration along characteristic curves. Numerical results for the dam-failure problem in cartesian and cylindrical coordinates are presented. The results are shown to be satisfactory. The Random Choice Method has the advantage of describing the breakdown of discontinuities in shallow water theory without need of ad hoc techniques and without introducing numerical diffusion and dispersion.

1. INTRODUCTION

In a previous work [9] the Random Choice Method (RCM) was applied to the numerical solution of a homogeneous hyperbolic system of conservation laws in one dimensional shallow water theory. In the present work we extend the method to include nonconservation forms of the shallow water equations, i.e., inhomogeneous systems such as those resulting from the consideration of friction effects or radial flows. A brief version of this work was presented in [10].

In the RCM the solution of the equations is constructed as a superposition of local theoretical solutions of Riemann problems and sampling techniques. This method was

* Present address: The Rockefeller University, 1230 York Avenue, N.Y. 10021.
† Present address: Institute of Hydraulic Research, University of Iowa, Iowa City, Iowa 52242.

0021-9991/81/110167-22$02.00/0

introduced by Glimm [7] and developed for gas dynamics by Chorin [2–4]. Sod [14] extended the RCM to a nonconservation form in gas dynamics.

The RCM is particularly efficient for the treatment of discontinuities that arise naturally in the solution of nonlinear hyperbolic equations (see, for instance, Lax [8]). The main problem in the application of the RCM resides in the solution of the Riemann problem. This becomes even more complex when inhomogeneous terms are present. Sod [14] avoided this difficulty by using a splitting technique consisting in a two-step procedure. In the first step the inhomogeneous term is removed and the resulting conservation form system is solved by the RCM. That is, first, the Riemann problem for the homogeneous system is solved, and then this solution is sampled. In the second step a system of ordinary differential equations is solved in a deterministic way by finite differences using as initial conditions the solution obtained in the first step. Later, Sod [15] recognizes that randomness should be introduced in the second step in order to obtain a solution which is in phase with the one obtained in the first step.

In the present work, following the tradition of Glimm's method, we first approximate the solution locally by solving Riemann problems for the inhomogeneous system using a numerical method to integrate the characteristic curves; then this solution is sampled. In this way there is no out-of-phase problem.

The solution of the Riemann problem for the shallow water equations is studied through the superposition of the two nonlinearly interacting scalar waves stemming from the shallow water system written in characteristic form. This original approach illuminates and simplifies the analysis of wave interactions.

The paper is organized as follows: (a) the main features of nonconservation forms and the procedures for their numerical solution are introduced with a simple inhomogeneous scalar wave equation; (b) a simplified linear homogeneous shallow water system is presented in order to illustrate the above-mentioned superposition technique; (c) the one dimensional shallow water system with slope and/or friction terms is considered and, finally, (d) the shallow water equations for radially symmetric flows are studied.

Numerical results are presented for: (1) a nonlinear scalar wave equation with a friction-like term; (2) the dam-failure problem, taking into account friction and slope effects; and (3) the problem of dam failure in a contracting channel section, considered as an example of a radial flow.

2. The Scalar Wave Equation

A simple example of a nonconservation form is provided by the following scalar wave equation:

$$U_t + F(U)_x + G(U) = 0, \tag{1}$$

where $F(U)$ is a flux density, $G(U)$ is a sink term, U is a scalar quantity and x and t

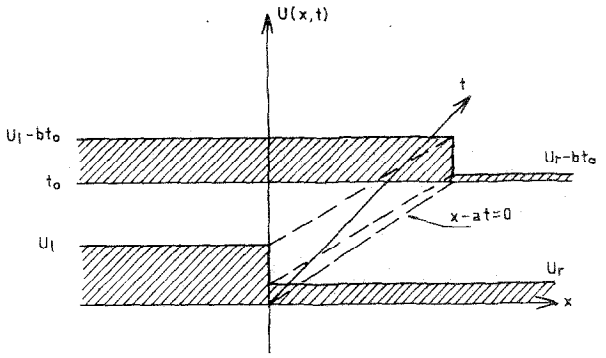

FIG. 1. Solution of the nonconservation Riemann problem for Eq. (1), case (a).

are the space and time coordinates. The initial conditions for the nonconservation Riemann problem are given by

$$\begin{aligned} U(x,0) = f(x) &= U_l \qquad \text{for} \quad x < 0, \\ &= U_r \qquad \text{for} \quad x > 0, \end{aligned} \tag{2}$$

where U_l and U_r are constants.

The main features of a nonconservation form appear in the following simple cases which we consider:

(a) $F(U) = aU$ and $G(U) = b$, a and b positive constants.

The solution of Eq. (1) with initial condition (2) is then

$$U(x,t) = f(x - at) - bt, \tag{3}$$

which is illustrated in Fig. 1. The wave propagates along characteristic lines with slope $1/a$, its value diminishing linearly due to the presence of the sink term.

(b) $F(U) = aU$ and $G(U) = bU$, a and b positive constants.

The solution of Eqs. (1), (2) is now

$$U(x,t) = f(x - at)\, e^{-bt}, \tag{4}$$

as shown in Fig. 2. The wave propagates along characteristic lines with slope $1/a$, its value diminishing exponentially due to the presence of the sink (or friction like) term.

(c) $F(U) = U^2/2$ and $G(U) = bU$, b a positive constant.

Equation (1) can be written now in characteristic form as

$$dU/dt = -bU \qquad \text{if} \quad dx/dt = U. \tag{5}$$

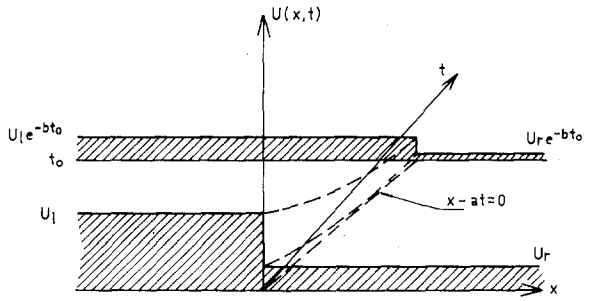

FIG. 2. Solution of the nonconservation Riemann problem for Eq. (1), case (b).

The solution of Eq. (5) along characteristic lines could be written as

$$U(x, t) = f\left(x - \int U\,dt\right) e^{-bt} \qquad \text{along} \quad x - \int U\,dt = \text{const.} \tag{6}$$

Expressions (5) and (6) indicate that in the smooth part of the flow, an initial condition will propagate along characteristic curves with slope $1/u$, its value decreasing exponentially due to the friction term.

As a result of the nonlinear character of Eq. (1), any initial discontinuity will break down into a simple centered wave. For the initial condition (2), if $U_1 < U_r$, the centered wave is a rarefaction wave, and if $U_1 > U_r$, the centered wave is a shock with velocity

$$s = 1/2(U_1 + U_r)\, e^{-bt}, \tag{7}$$

by the Rankine–Hugoniot condition [8]. Both cases are illustrated in Fig. 3.

In the following the numerical procedure used to integrate the shallow water system is introduced by means of its application to the scalar wave equation for case (c). Since the RCM is first order accurate, the integration of Eq. (5) can be approximated by

$$U(x(\Delta t), \Delta t) = (1 - b\,\Delta t)\, U_0 + O(\Delta t^2), \tag{8a}$$

$$x(\Delta t) = x(0) + U_0 \Delta t + O(\Delta t^2), \tag{8b}$$

where $U_0 = U(x(0), 0)$. Equation (8a) shows that making $\Delta t = 0$ is equivalent to making $b = 0$, thus U_0 coincides with the known solution for $b = 0$. This is to say that the breakdown of an initial discontinuity is independent of the friction term. Therefore, the characteristic curves for $b = 0$ and $b \neq 0$ are tangent to each other when $t = 0$ (see Fig. 4). Equation (8b) shows that the curvature of the characteristic curves for $b \neq 0$ can be neglected to first order in Δt so that the two characteristic families (for $b = 0$ and $b \neq 0$) are coincident. From the foregoing, the solution for $t = \Delta t$ can be calculated for any desired value of x.

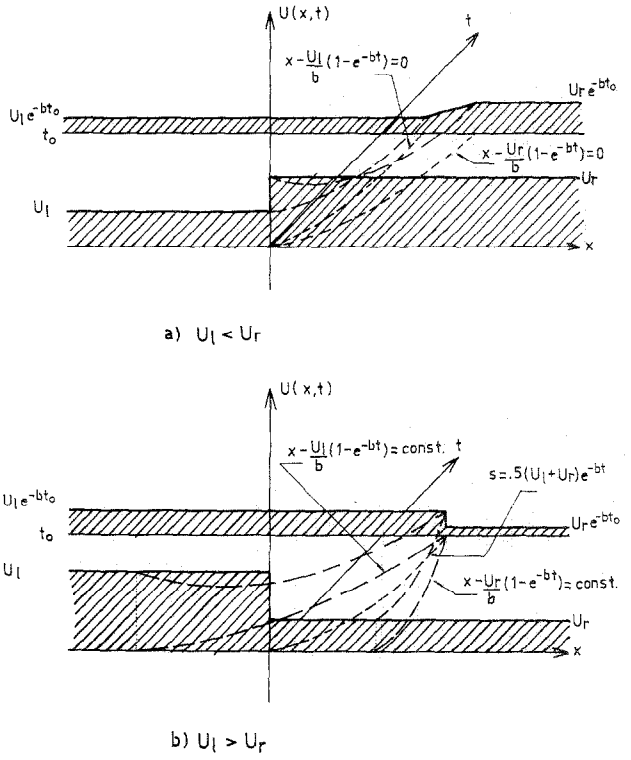

FIG. 3. Solution of the nonconservation Riemann problem for Eq. (1), case (c).

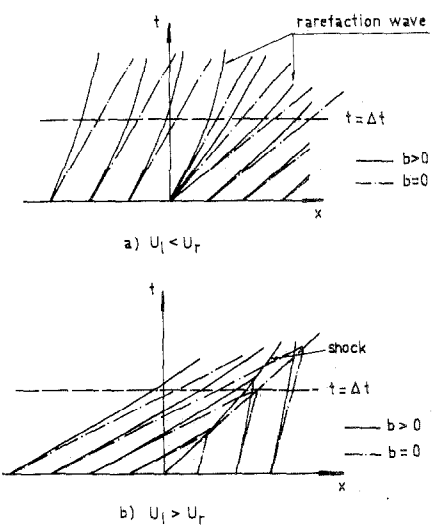

FIG. 4. Characteristic curves for Eq. (1), case (c).

For sampling the Riemann solution we have used the binary van der Corput equidistributed quasi-random sampling procedure proposed by Collela. For a discussion of the merits of this procedure see [5].

It is worth noting that for the case of the inhomogeneous scalar wave equation, the method described is in fact equivalent to that of Sod [15]. This is no longer true for the shallow water system.

It can be proved that the extended RCM here introduced is convergent when applied to a linear inhomogeneous scalar wave equation. Chorin [4] demonstrated the convergence of the RCM for the case of the linear scalar wave equation with initial discontinuous conditions. That demonstration is also valid for a linear inhomogeneous scalar wave equation because the inhomogeneous term has no influence on the slope of the characteristics, which remain straight lines. Therefore, the expected value of the position of the discontinuity of the approximate solution coincides with the theoretical value, and the variance of the position tends to zero as the mesh size is refined. However, the inhomogeneous term affects the value of the solution. Its influence is calculated through a numerical integration procedure which converges to the theoretical solution when the mesh is refined.

Figure 5 shows the numerical solution by the RCM of Eq. (1), case (c), for the

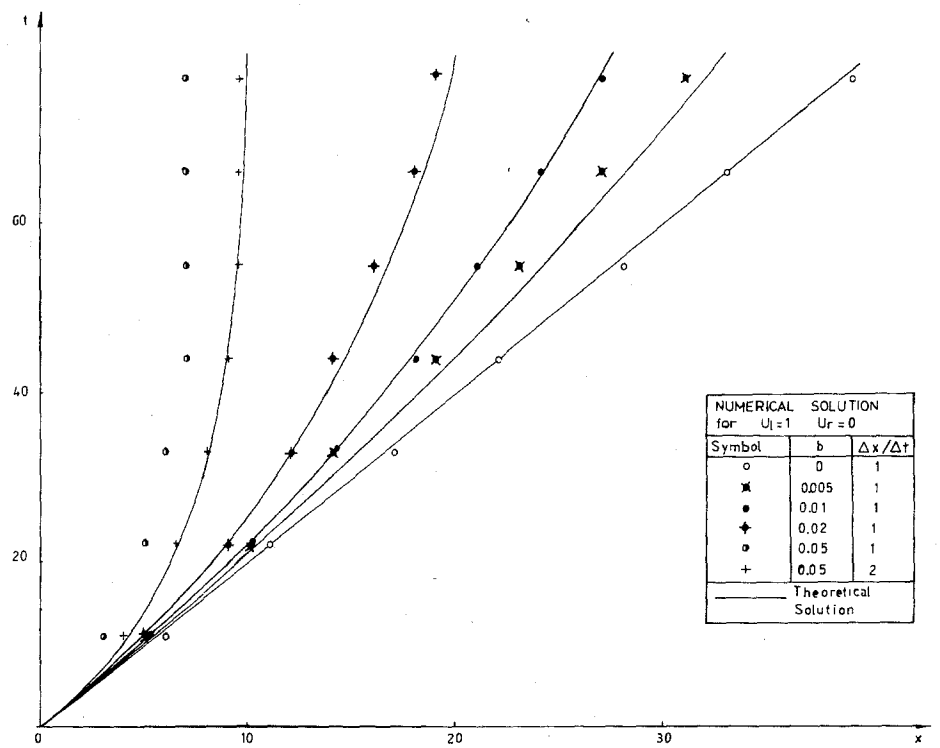

FIG. 5. Solution of Eq. (1), case (c) by the RCM.

trajectory of a shock moving to the right. The solution for different values of b is compared with the theoretical solution given in Eq. (7). There is good agreement except for the largest value of b, but since the solution is a function of the product $b\,\Delta t$, it can be improved by decreasing Δt. This is done in Fig. 5, where, by halving the time step, an excellent result is obtained for the largest value of b.

3. A Simplified Shallow Water System

A simple linear model of the shallow water system is given by expression (1), where now

$$U = \begin{bmatrix} h \\ u \end{bmatrix}; \qquad F(U) = C \begin{bmatrix} u \\ h \end{bmatrix}; \qquad G(U) = 0, \tag{9}$$

with h and u being scalar quantities and C a positive constant. System (1)–(9) written in characteristic form becomes

$$\frac{d}{dt}(h+u) = 0 \qquad \text{if} \quad \frac{dx}{dt} = C, \tag{10a}$$

$$\frac{d}{dt}(h-u) = 0 \qquad \text{if} \quad \frac{dx}{dt} = -C. \tag{10b}$$

There are two families of characteristic lines with slope $\pm C$. Along each of them the quantities $r = h + u$ and $s = h - u$ are constant, respectively; r and s are called Riemann invariants. System (10a), (10b) can be written in the alternative form

$$\frac{dW}{dt} = 0 \qquad \text{if} \quad I\frac{dx}{dt} = A, \tag{11}$$

where I is the identity matrix, and

$$W = \begin{bmatrix} r \\ s \end{bmatrix} \qquad \text{and} \qquad A = \begin{bmatrix} C & 0 \\ 0 & -C \end{bmatrix}. \tag{12}$$

System (11), (12) can be interpreted as the equations for two independent scalar waves: the "r" and the "s" waves. Therefore it is useful to examine system (1)–(9) by studying the superposition of the r and s waves of system (11), (12). The initial conditions for the Riemann problem are given by

$$W(x,0) = \begin{bmatrix} H_1(x) \\ H_2(x) \end{bmatrix} = \begin{cases} \begin{bmatrix} r_l \\ s_l \end{bmatrix} & \text{for} \quad x < 0, \\ \begin{bmatrix} r_r \\ s_r \end{bmatrix} & \text{for} \quad x > 0. \end{cases} \tag{13}$$

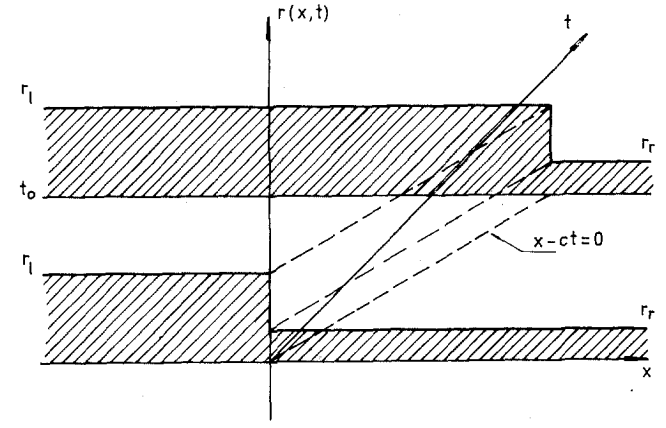

a) r wave

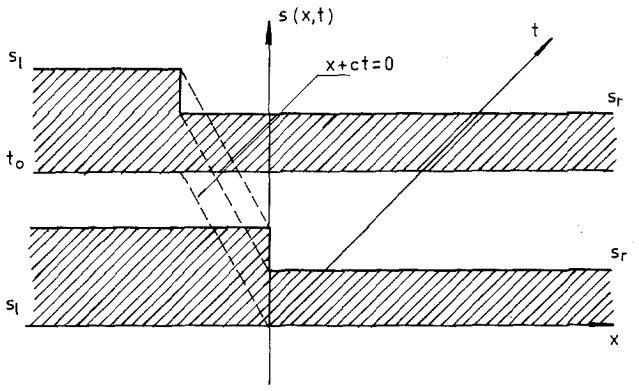

b) s wave

FIG. 6a–6d. Solution of the Riemann problem for Eqs. (11), (12).

The solution of Eqs. (11), (12) with initial conditions (13) is

$$W(x, t) = \begin{bmatrix} H_1(x - Ct) \\ H_2(x + Ct) \end{bmatrix}, \tag{14}$$

as illustrated in Figs. 6a and b. The r wave propagates unchanged along characteristic lines with slope $1/C$, while the s wave propagates unchanged along characteristic lines with slope $-1/C$.

We can now solve for the variables h and u by superposing the r and the s waves. We obtain (Figs. 6c and d),

$$h(x, t) = \frac{r + s}{2} = 1/2[H_1(x - Ct) + H_2(x + Ct)] \tag{15}$$

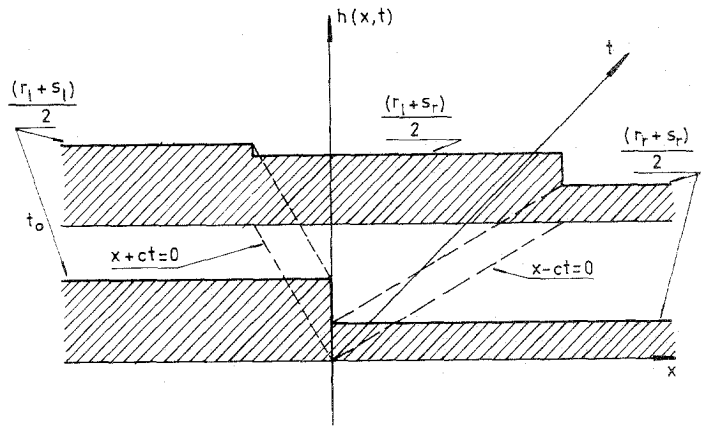

c) h

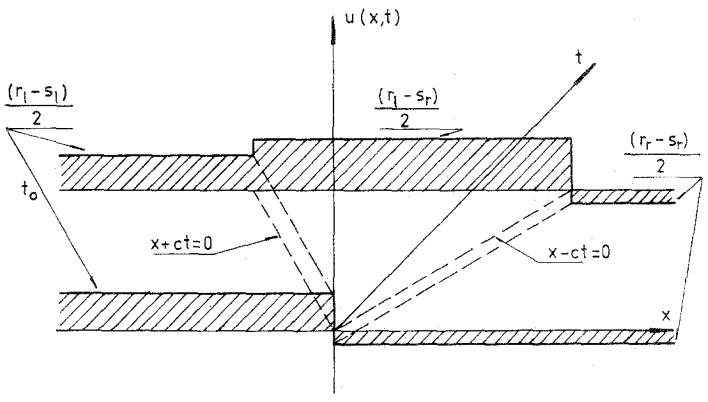

d) u

FIG. 6—*Continued.*

$$u(x,t)=\frac{r-s}{2}=1/2[H_1(x-Ct)-H_2(x+Ct)]. \tag{16}$$

This procedure will be applied in the solution of the shallow water system.

4. THE SHALLOW WATER SYSTEM

The one dimensional shallow water system is given by expression (1), where

$$U=\begin{bmatrix} uh \\ h \end{bmatrix}, \qquad F(U)=\begin{bmatrix} u^2h+gh^2/2 \\ uh \end{bmatrix}, \qquad \text{and} \qquad G(U)=\begin{bmatrix} -hR(U) \\ 0 \end{bmatrix}. \tag{17}$$

Here u is the water velocity, h is the depth, g is the gravity and $R(U)$ is a friction term and/or a slope term. System (1)–(17) can be written in characteristic form as (see Stoker [16])

$$\frac{d}{dt}[u + 2(gh)^{1/2}] = R(U) \qquad \text{if} \quad \frac{dx}{dt} = u + (gh)^{1/2}, \tag{18a}$$

$$\frac{d}{dt}[u - 2(gh)^{1/2}] = R(U) \qquad \text{if} \quad \frac{dx}{dt} = u - (gh)^{1/2}. \tag{18b}$$

As in the case of the inhomogeneous scalar wave equation, the breakdown of an initial discontinuity in the shallow water system is independent of the effect of the friction terms (see Dressler [6]). Therefore, the breakdown process is analyzed by applying the superposition procedure of Section 3 to the homogeneous shallow water system. Equations (18a), (18b) for $R(U) = 0$ indicate that the quantities $r, s = u \pm 2(gh)^{1/2}$ are constant along characteristic lines with slope $u \pm (gh)^{1/2}$, respectively; r and s are the corresponding Riemann invariants. System (18a), (18b) for $R(U) = 0$ can be written as

$$\frac{dW}{dt} = 0 \qquad \text{if} \quad I\frac{dx}{dt} = A, \tag{19}$$

where I is the identity matrix, and

$$W = \begin{bmatrix} r \\ s \end{bmatrix} \qquad \text{and} \qquad A = \begin{bmatrix} (3r+s)/4 & 0 \\ 0 & (r+3s)/4 \end{bmatrix}. \tag{20}$$

Next the shallow water system (1)–(17) for $R(U) = 0$ is analyzed by superposing the r and s scalar waves of system (19), (20). The initial conditions for the Riemann problem are given by

$$W(x, 0) = \begin{cases} W_l = \begin{bmatrix} r_l \\ s_l \end{bmatrix} & \text{for} \quad x < 0, \\ W_r = \begin{bmatrix} r_r \\ s_r \end{bmatrix} & \text{for} \quad x > 0, \end{cases} \tag{21}$$

and we distinguish the following cases (see Fig. 7):

(i) $r_l < r_r$ and $s_l = s_r$.

In this case a right r depression wave is obtained, while s remains constant;

(ii) $r_l = r_r$ and $s_l < s_r$.

In this case a left s depression wave is obtained, while r remains constant;

(iii) $r_l < r_r$ and $s_l < s_r$.

In this case both a right r and a left s depression wave are obtained.

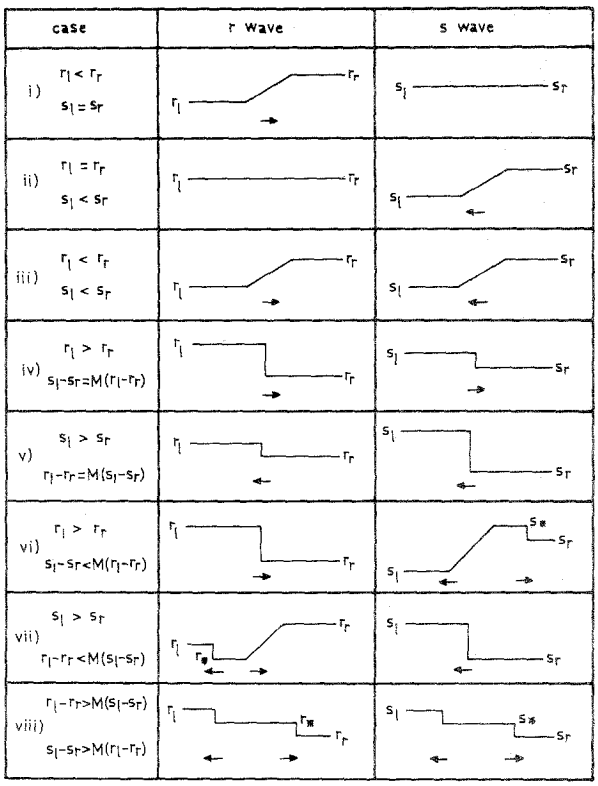

FIG. 7. Solution of the Riemann problem for the r and s waves when $R(U) = 0$.

In these three cases, one wave influences the other by producing a constant contribution to the velocity of propagation.

(iv) $r_1 > r_r$ and $s_1 - s_r = M(r_1 - r_r)$, where

$$M = \frac{K_0 - 1}{K_0 + 1}; \quad K_0 = K(r_1 - s_1, r_r - s_r); \quad K(x, y) = \frac{\sqrt{2}}{4} \frac{(x + y)}{xy} \sqrt{x^2 + y^2}. \quad (22)$$

Statement (22) verifies that $0 \leqslant M < 1$, with $M = 0$ for $x = y$ (this equation is obtained from the Rankine–Hugoniot relations [12]). In this case a right r shock and a right s shock wave are obtained.

(v) $s_1 > s_r$ and $r_1 - r_r = M(s_1 - s_r)$.

In this case a left s shock and a left r shock wave are obtained.

(vi) $r_1 > r_r$ and $s_1 - s_r < M(r_1 - r_r)$.

In this case a right r shock wave and an s wave composed of a left depression and a right shock wave are obtained. The right s shock appears even in the case $s_1 = s_r$ as a result of nonlinear interaction with the r wave.

(vii) $s_1 > s_r$ and $r_1 - r_r < M(s_1 - s_r)$.
In this case a left s shock wave and an r wave composed of a right depression and a left shock wave are obtained;

(viii) $r_1 - r_r > M(s_1 - s_r)$ and $s_1 - s_r > M(r_1 - r_r)$.
In this case left and right r and s shock waves are obtained.

The intermediate states r_* and s_* appearing in cases (vi), (vii) and (viii) as a result of the nonlinear interaction must be calculated through an iteration procedure (e.g., the Godunov iteration; see, for instance [12]).

The solutions for the variables u and h corresponding to the cases considered above are shown in Fig. 8. Here $h_1 = (r_1 - s_1)^2/(16g)$, $u_1 = (r_1 + s_1)/2$, $h_r = (r_r - s_r)^2/(16g)$ and $u_r = (r_r + s_r)/2$. The foregoing analysis is the basis for the solution of the Riemann problem for the inhomogeneous shallow water system.

Equations (18a), (18b) for the general case $R(U) \neq 0$ can be written in the alternate form

$$\frac{dW}{dt} = H(W) \qquad \text{if} \quad I\frac{dx}{dt} = A, \tag{23}$$

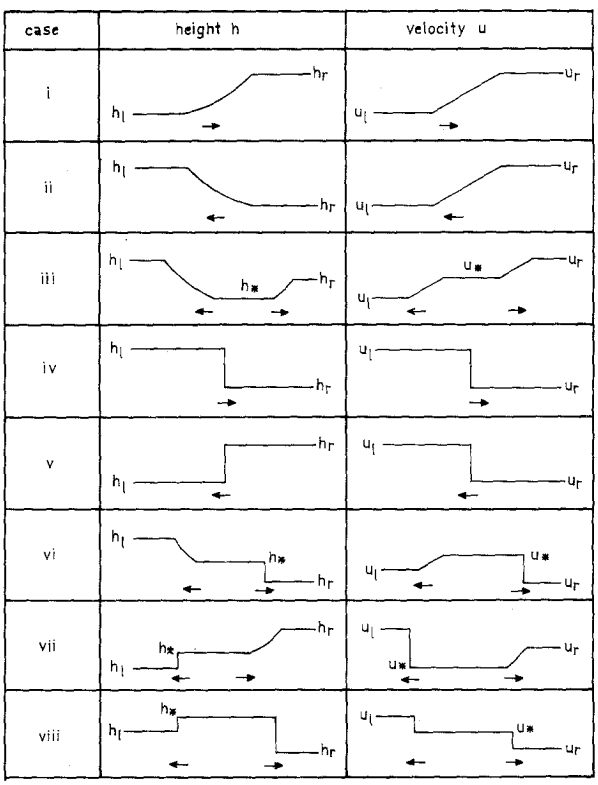

FIG. 8. Solution of the Riemann problem for the variables h and u when $R(U) = 0$.

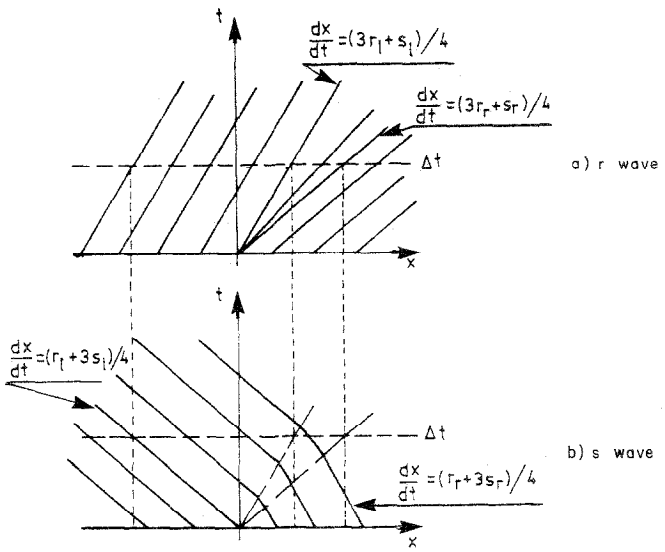

FIG. 9. Characteristic curves for case (i).

where W and A are given in (20) and

$$H(W) = \begin{bmatrix} R(U(W)) \\ R(U(W)) \end{bmatrix}. \tag{24}$$

In spite of not being Riemann invariants, the quantities r and s can still be interpreted as two nonlinearly interacting scalar waves, the superposition of which gives the solution for the variables u and h.

The nonconservation Riemann problem posed in Eqs. (18)–(21) is solved by integrating along characteristic curves, taking into consideration that since the RCM is first order accurate, the characteristic curves for each wave coincide with the corresponding curves for $R(U(W)) = 0$. The integration process is different for each one of the eight cases analyzed above. We give the details of this procedure.

Case (i) $r_l < r_r$ and $s_l = s_r$. For this case the characteristic curves for each wave are shown in Fig. 9. Four regions can be distinguished:

(1) $x < (r_l + 3s_l)\,\Delta t/4$.

The integration of Eqs. (20)–(23), (24) for W gives

$$r(x, \Delta t) = r_l + R_l\,\Delta t + O(\Delta t^2), \tag{25a}$$

$$s(x, \Delta t) = s_l + R_l\,\Delta t + O(\Delta t^2), \tag{25b}$$

where $R_l = R(U(W_l))$. Thus, in this region, it follows from Eqs. (25a), (25b) and from definitions of r and s that

$$u(x, \Delta t) = u_1 + R_1 \Delta t + O(\Delta t^2), \tag{26a}$$

$$h(x, \Delta t) = h_1 + O(\Delta t^2). \tag{26b}$$

(2) $x > (3r_r + s_r)\Delta t/4$.
In this region, considerations similar to those just given lead to

$$u(x, \Delta t) = u_r + R_r \Delta t + O(\Delta t^2), \tag{27a}$$

$$h(x, \Delta t) = h_r + O(\Delta t^2), \tag{27b}$$

where $R_r = R(U(W_r))$.

(3) $(r_1 + 3s_1)\Delta t/4 < x < (3r_1 + s_1)\Delta t/4$.
In this region the integration of Eqs. (20)–(23), (24) for W yields

$$r(x, \Delta t) = r_1 + R_1 \Delta t + O(\Delta t^2), \tag{28a}$$

$$s(x, \Delta t) = s_r + R_r \Delta t + O(\Delta t^2), \tag{28b}$$

so that

$$u(x, \Delta t) = u_1 + (R_1 + R_r)/2\,\Delta t + O(\Delta t^2), \tag{29a}$$

$$c(x, \Delta t) = c_1 + (R_1 - R_r)/4\,\Delta t + O(\Delta t^2), \tag{29b}$$

where $c = (gh)^{1/2}$.

(4) $(3r_1 + s_1)\Delta t/4 < x < (3r_r + s_r)\Delta t/4$.
In this region the integration for the s wave is the same as before; i.e., it is given by Eq. (28b), but the integration for the r wave yields

$$r(x, \Delta t) = r_0 + R_0 \Delta t + O(\Delta t^2), \tag{30}$$

where

$$R_0 = R(U(W_0)), \qquad W_0 = \begin{bmatrix} r_0 \\ s_r \end{bmatrix}. \tag{31}$$

Here r_0 represents the centered depression wave for $R(U(W)) = 0$. It now follows from Eqs. (30)–(31) that, in this region,

$$u(x, \Delta t) = u_0 + (R_0 + R_r)/2\,\Delta t + O(\Delta t^2), \tag{32a}$$

$$c(x, \Delta t) = c_0 + (R_0 - R_r)/4\,\Delta t + O(\Delta t^2), \tag{32b}$$

where $u_0 = (r_0 + s_r)/2$ and $c_0 = (r_0 - s_r)/4$.

Cases (ii) and (iii) can be treated in a manner similar to that for case (i).

Case (iv) $r_1 > r_r$ and $s_1 - s_r = M(r_1 - r_r)$. In this case the characteristic curve for each wave are shown in Fig. 10. We study case (iv) in three regions separately:

(1) $x < (r_1 + 3s_1)\,\Delta t/4$.

In this region the solution is the same as in case (i); i.e., it is given by Eqs. (26a), (26b).

(2) $x > \bar{U}\,\Delta t$, where

$$\bar{U} = u_r + 1/4(r_1 - s_1)/(r_r - s_r)\{1/2[(r_1 - s_1)^2 + (r_r - s_r)^2]\}^{1/2} \tag{33}$$

is the velocity of propagation of the shock for $R(U(W)) = 0$ (this follows from the Rankine–Hugoniot relations). In this region the solution is analogous to the solution in region 2 of case (i); i.e., it is given by Eqs. (27a), (27b).

(3) $(r_1 + 3s_1)\,\Delta t/4 < x < \bar{U}\,\Delta t$.

In this region the integration of the r wave is the same as for region 3 of case (i); i.e., it is given by Eq. (28a), but the integration of the s wave must be divided into two parts due to the discontinuity present in the shock trajectory. For the s wave (see Fig. 10),

$$s(x, \Delta t) = s_A + R_A(\Delta t - \Delta t_A), \tag{34a}$$

$$s_B = s_r + R_r\,\Delta t_A, \tag{34b}$$

where the subindexes A and B denote values just to the left and to the right of the shock trajectory, respectively. The relation between s_A and s_B is given by

$$s_A - s_B = (K_1 - 1)/(K_1 + 1)(r_A - r_B). \tag{34c}$$

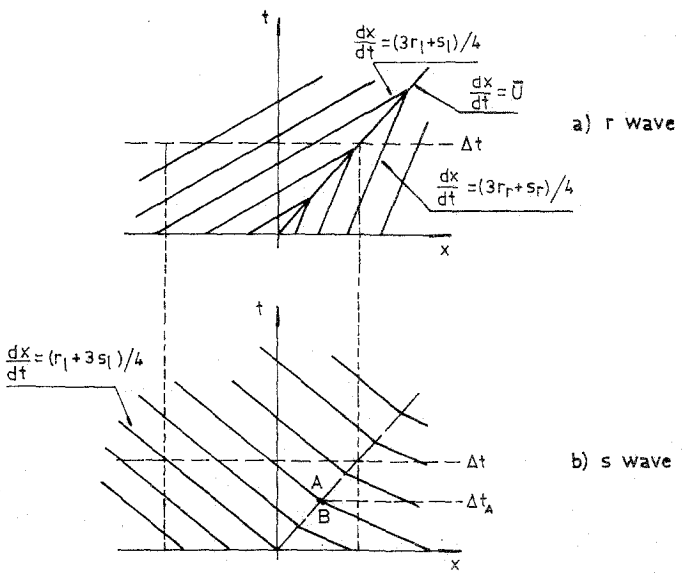

FIG. 10. Characteristic curves for case (iv).

Here $K_1 = K(r_A - s_A, r_B - s_B)$ and r_A and r_B must be calculated by integration. For r_A and r_B we have

$$r_A = r_1 + R_1 \Delta t_A, \tag{34d}$$

$$r_B = r_r + R_r \Delta t_A, \tag{34e}$$

where Δt_A can be computed directly from

$$\Delta t_A = \frac{x - (r_1 + 3s_1)\Delta t/4}{\bar{U} - (r_1 + 3s_1)\Delta t/4}. \tag{34f}$$

Equations (34a)–(34c) with three unknowns ($s(x, \Delta t)$, s_A, s_B) can be solved in $O(\Delta t)$ to obtain $s(x, \Delta t)$. The result is

$$s(x, \Delta t) = s_1 + R_1(\Delta t - \Delta t_A) + \alpha \Delta t_A, \tag{35}$$

where

$$\alpha = \frac{R_r + (K_0 - 1)/(K_0 + 1)(R_1 - R_r) + 2\dot{K}_0/(K_0^2 - 1)(s_1 - s_r) R_1}{1 + 2\dot{K}_0/(K_0^2 - 1)(s_1 - s_r)}$$

with

$$\dot{K}_0 = \frac{\partial K}{\partial x}(r_1 - s_1, r_r - s_r).$$

From Eqs. (28a) and (35) it follows that

$$u(x, \Delta t) = u_1 + [R_1(2\Delta t - \Delta t_A) + \alpha \Delta t_A]/2, \tag{36a}$$

$$c(x, \Delta t) = c_1 + (R_1 \Delta t_A - \alpha \Delta t_A)/4. \tag{36b}$$

Case (v) can be treated in a manner similar to that for case (iv), while cases (vi) and (vii) are combinations of previous cases. Case (viii) is somewhat different. In case (viii), both the integration of the r and s waves in the central region must be divided into two parts, and a process of reflection of information occurs between the two shock trajectories. This leads to an infinite sequence of equations that successively introduce new unknowns corresponding to points which approach zero. For calculation purposes this sequence can be truncated when the points are within a time interval $O(\Delta t^2)$ from the origin, assigning to these latter points the values of the known solution for $R(U(W)) = 0$.

The sampling technique for the Riemann solution is the same as for the scalar wave equation. Moreover the extended RCM so far discussed is convergent when applied to a linear inhomogeneous shallow water system. In effect, if the linear inhomogeneous shallow water system is analyzed in terms of the corresponding r and s waves, the proof is the same as in the scalar case.

Numerical solutions for the shallow water system obtained with the RCM are now shown. In Fig. 11 the results for the dam-failure problem with friction effects are presented, together with the theoretical solutions for the case without friction. The initial conditions are: $h = 10$ m, $u = 0$ for $x < 0$ and $h = 2$ m, $u = 0$ for $x > 0$. The friction term is given by $R(U) = -gu^2/(C^2h)$, where $C = 52\ \mathrm{m}^{1/2}/\mathrm{sec}$. is the Chezy coefficient. It can be seen that the friction effects are initially concentrated in the shock region, damping and decelerating the shock; for larger times these effects spread upstream, so the heights increase (and the velocities decrease).

In Fig. 12 the results for the dam-failure problem with a constant bottom slope and without friction are shown. The initial conditions are the same as in the previous example and the slope term is given by $R(U) = gS_0$, where $S_0 = 0.0004$ is the bottom slope. It can be observed that the velocities, including the shock velocity, increase uniformly and constantly due to the slope influence, while the heights remain unchanged.

In Fig. 13 a comparison is made with the numerical results obtained by Sakkas and Strelkoff [13] by the method of characteristics, for the case of the dam break flood on a dry horizontal bed. The initial conditions are $h = 0.11$ m, $u = 0$ for $x < 0$. As our algorithm cannot deal with a zero height, we have taken $h = 10^{-5}$ m, $u = 0$ for $x > 0$. The friction term is given by $R(U) = -gn^2u^2/h^{4/3}$, where $n = 0.0166$ is the Manning coefficient. Although these are the least favorable conditions for the RCM, the heights and velocities calculated by the RCM are in good agreement with those obtained by Sakkas and Strelkoff [13].

In Fig. 14 a comparison is made with the numerical results obtained by Ré [11]

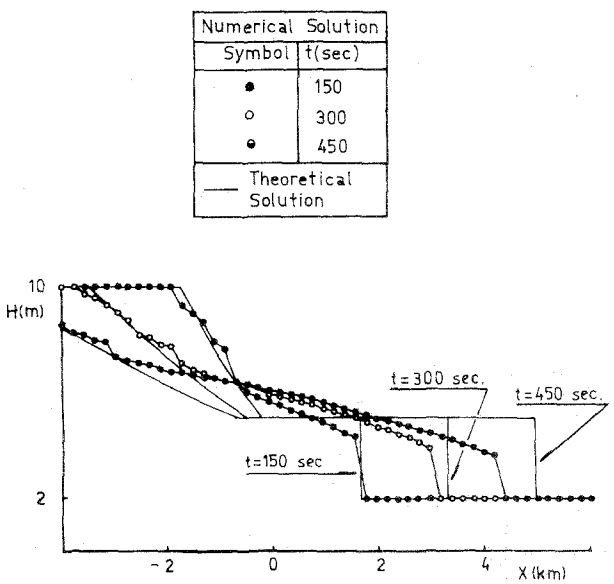

FIG. 11. The dam-failure problem with friction effects as calculated with the RCM.

for the dam-failure problem with friction and slope effects using finite differences on the characteristic equations. The initial conditions are $h = 1.8$ m, $u = 1.6$ m/sec for $x > 0$, and h and u are as given by Ré [11] for $x < 0$. The inhomogeneous term is given by $R(U) = g[S_0 - u^2/(C^2h)]$, where $S_0 = 0.0009$ and $C = 40\ \text{m}^{1/2}/\text{sec}$. It is observed that the results obtained with the RCM are very close to those given by Ré [11].

The agreement shown between the results of the RCM and those of the characteristic finite difference method (another method well-suited for treating discon-

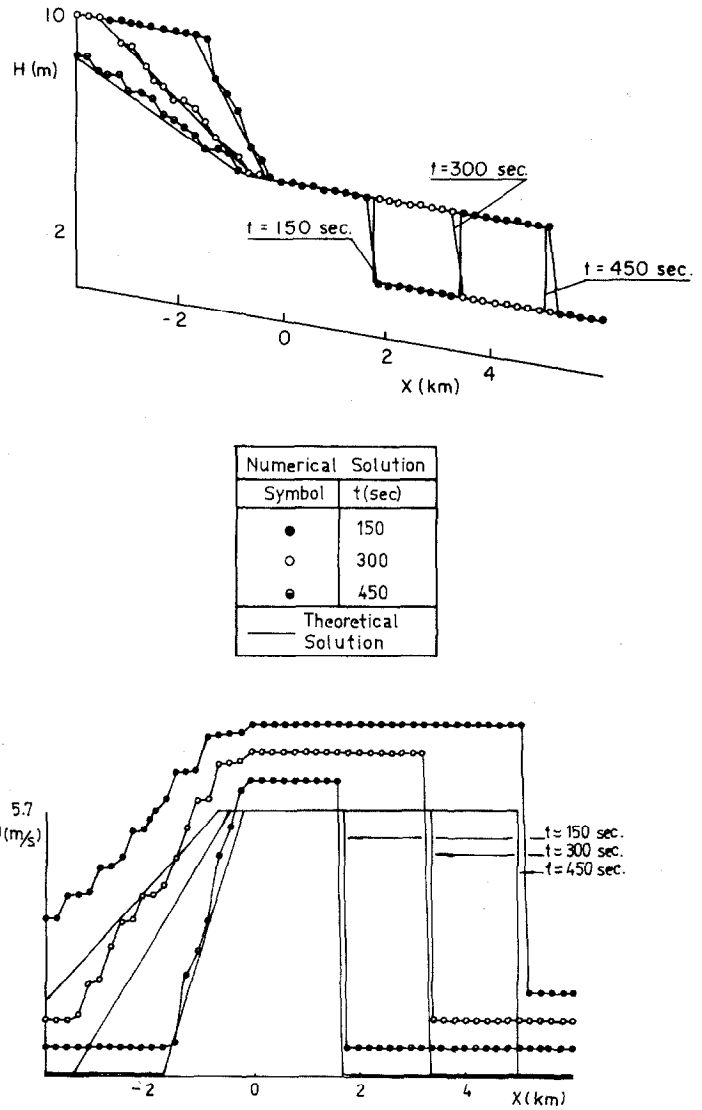

FIG. 12. The dam-failure problem with slope effects as calculated with the RCM.

tinuities), evidences a similar degree of accuracy. The advantages of the RCM are that there is no need for a separate treatment of discontinuities and one can use a fixed rectangular mesh. Furthermore, the RCM automatically accounts for the spontaneous formation of shocks without introducing numerical diffusion and dispersion.

The numerical calculations and figures presented above were made in a PDP 11/45

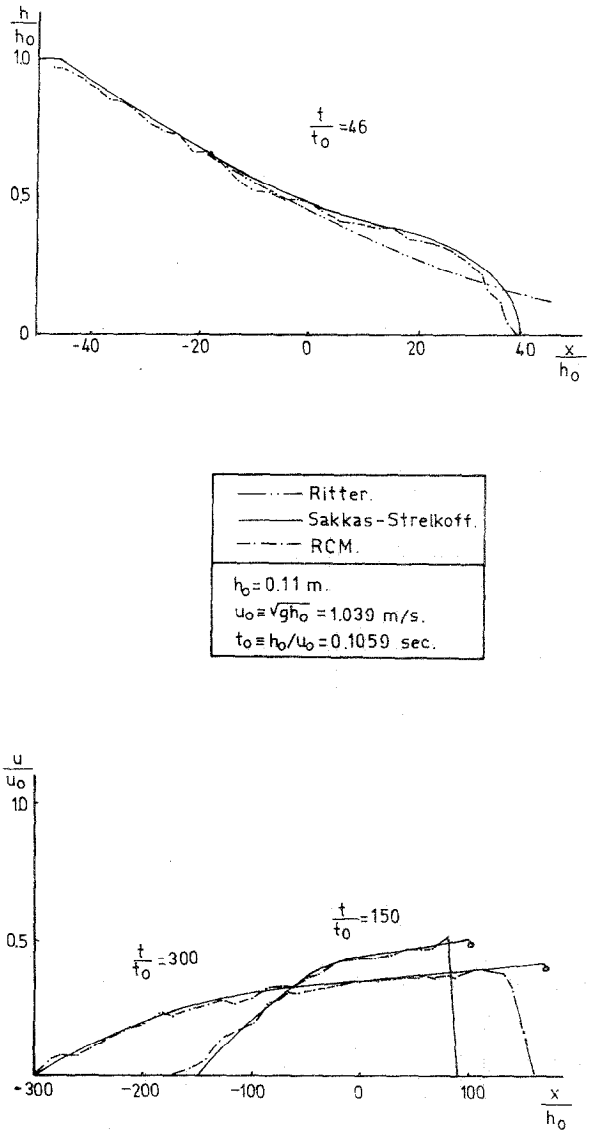

FIG. 13. Comparison of results for the dam break flood on a dry bed.

digital equipment (48K bytes, Fortran compiler), with a plotting device. All the runs were made with a mesh of 51 points. The CPU time per cycle was estimated at 2.4 sec.

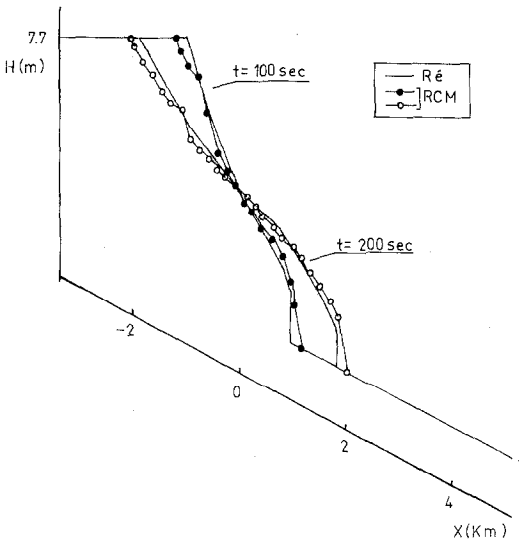

FIG. 14. Comparison of results for the dam failure with friction and slope.

5. RADIAL SHALLOW WATER FLOW

The one dimensional shallow water system for cylindrically symmetric shallow water flows without friction and slope terms is given by expression (1) (see Abbott [1]), where now x is the cylindrical radial coordinate, and

$$U=\begin{bmatrix} xuh \\ xh \end{bmatrix}; \qquad F(U)=\begin{bmatrix} xu^2h \\ xuh \end{bmatrix}; \qquad \text{and} \qquad G(U)=\begin{bmatrix} x(gh^2/2)_x \\ 0 \end{bmatrix}. \tag{37}$$

System (1)–(37) can be written in the alternate form

$$\frac{dW}{dt}=H(W) \qquad \text{if} \quad I\frac{dx}{dt}=A, \tag{38}$$

where W and A are given in expression (20), and

$$H(W)=\begin{bmatrix} -R(U) \\ R(U) \end{bmatrix}, \qquad R(U)=\frac{(r+s)[\,g(r-s)]^{1/2}}{4x}. \tag{39}$$

The nonconservation Riemann problem for the r and s waves is given by expressions (38)–(21). As the numerical integration process along characteristic curves does not

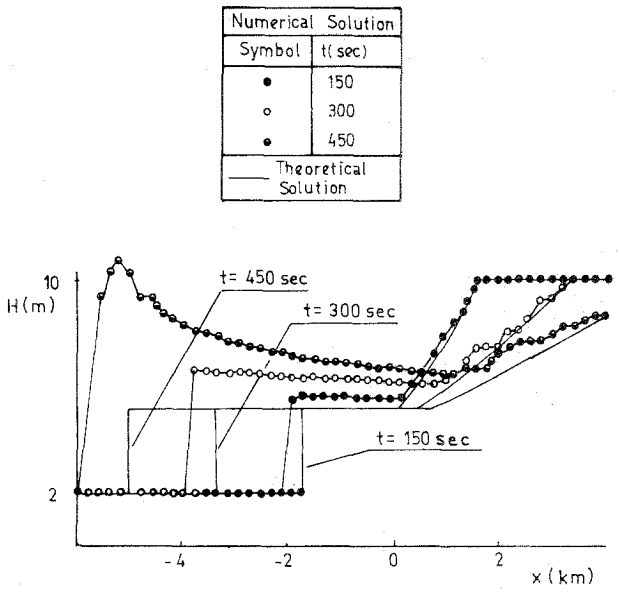

FIG. 15. The dam break wave through a contracting channel section, as calculated by the RCM.

differ essentially from the previous one dimensional shallow water problem, it is not examined here.

In practice the flow through an expanding or contracting channel section could be analyzed as a radial flow. In Fig. 15 the result for the dam break wave through a contracting channel section is shown, together with the theoretical solution for the case of one dimensional motion. The initial conditions are: $h = 2$ m, $u = 0$ for $x < 0$ and $h = 10$ m, $u = 0$ for $x > 0$. The flow converges toward the point located at the extreme left of the figure. It can be observed that due to the radial movement, the heights and velocities increase.

6. CONCLUSIONS

The range of application of the RCM has been extended to include nonconservation forms of the equations of shallow water theory. Moreover the nonconservation Riemann problem has been analyzed with a method based on the superposition of two scalar wave equations. This approach clarifies the complex nonlinear process inherent in the shallow water system. The solution of the nonconservation Riemann problem is obtained by means of a numerical integration along characteristic curves.

Numerical solutions for the dam-failure problem in cartesian and cylindrical coordinates are also presented. The significant effects of the inhomogeneous terms are evidenced by the difference between the homogeneous and inhomogeneous solutions.

The accuracy of the RCM has been assessed by comparing its results with those

obtained by characteristic finite difference methods. The RCM describes the wave interaction of shallow water theory with no need of ad hoc techniques and without introducing numerical diffusion and dispersion. The relative complexity of the RCM is more than balanced by its power of resolution for treating discontinuities and its unconditional stability which allows for a much coarser mesh size at the same level of accuracy.

The extension of the RCM to nonconservation forms of the equations of shallow water theory renders possible its application to a great variety of problems of practical interest, opening a wide avenue of research, not only in hydraulics, but also in meteorology, oceanography, and geophysical fluid dynamics in general.

REFERENCES

1. M. B. ABBOTT AND E. W. LINDEYER, *Houille Blanche*, No. 1 (1969) 65–70.
2. A. J. CHORIN, *J. Comput. Phys.* **22** (1976), 517–533.
3. A. J. CHORIN, *J. Comput. Phys.* **25** (1977), 253–272.
4. A. J. CHORIN AND J. E. MARSDEN, "A Mathematical Introduction to Fluid Mechanics," Springer–Verlag, New York, 1979.
5. P. COLLELA, "An Analysis of the Effect of Operator Splitting and of the Sampling Procedure on the Accuracy of Glimm's Method," Ph. D. thesis, University of California, Berkeley, Mathematics Department, 1979.
6. R. F. DRESSLER, *J. Res. Nat. Bur. Stand.* **49**, No. 3 (1952), 217–225.
7. J. GLIMM, *Comm. Pure Appl. Math.* **18** (1965), 697–715.
9. G. MARSHALL AND R. MENÉNDEZ, *J. Comput. Phys.* **39** (1981), 1–21.
10. G. MARSHALL AND N. MENÉNDEZ, *in* "Boundary and Interior Layers, Proceedings BAIL I Conf., Trinity College, Dublin, June (1980)" (J. J. H. Miller, Ed.), Boole, Dublin, 1980.
11. R. RÉ, *Houille Blanche* **3** (1946), 181–187.
12. R. D. RICHTMYER AND K. W. MORTON, "Finite Difference Methods for Initial Value Problems," Interscience, New York, 1967.
13. J. G. SAKKAS AND T. STRELKOFF, *J. Hydraul. Div., Amer. Soc. Civ. Engin.* **12** (1973), 2195–2216.
14. G. SOD, *J. Fluid Mech.* **83,** pt. 4 (1977), 787–794.
15. G. SOD, "A Hybrid Random Choice Method with Applications to Internal Combustion Engines," Springer Lecture Notes in Physics No. 90, p. 492, Springer–Verlag, Berlin/New York, 1979.
16. J. J. STOKER, "Water Waves," New York, Interscience, 1957.